Nano World Journal

https://doi.org/10.17756/nwj.2019-071

Research Article

Open Access

Monitoring of Diffraction Efficiency, During Replication Process of a Diffraction Grating on Convex Substrate by Solvent Vapor Assisted Imprinting Lithography

Georges Horugavye*, Bernard Sabushimike, and Serge Habraken

Spatial Technologies and Astrophysics Research (STAR) Institute, University of Liege, Belgium

*Correspondence to:
Georges Horugavye
Holography and Optical Laboratory (HOLOLAB), Spatial Technologies and Astrophysics Research (STAR) Institute
University of Liege Allée du six Août 19
4000 Liège, Belgium
E-mail: ghorugavye@doct.uliege.be

Received: October 01, 2019
Accepted: January 11, 2020
Published: January 13, 2020

Citation: Horugavye G, Sabushimike B, Habraken S. 2020. Monitoring of Diffraction Efficiency, During Replication Process of a Diffraction Grating on Convex Substrate by Solvent Vapor Assisted Imprinting Lithography. *NanoWorld J* 5(4): 41-48

Published by United Scientific Group

Abstract

For several reasons and in many fields, the replication of structures or nanostructures is realized. Actually, a lot of techniques exist, and the quality evaluation of the replication process is generally realized after replication process. In such conditions, the determination of adequate duration is a challenge. Diffraction grating replication realized by solvent vapor assisted imprinting lithography (SVAIL) process, on convex substrate, is here reported. Photoresist coating on convex substrate is also a challenge. It is treated in this paper before going on with replication and experimental measurement. Next, with that coated convex substrate, diffraction grating replication is realized. And the diffraction efficiency is monitored in real time during the replication process. The monitoring indicates the variation of diffraction efficiency during the evolution of SVAIL process. The comparison of monitored diffraction efficiency to theoretical simulations of diffraction efficiency for various steps of SVAIL process, allows to deduce the value of diffraction efficiency for optimal replication; and finally, the required duration of the replication process for optimal result is deduced.

Keywords

Monitoring, Replication, Diffraction, Grating, Solvent, Vapor, Convex, Substrate

Introduction

Diffraction gratings are key elements in imaging spectrometers. Diffraction gratings are generally fabricated on flat substrate. However, their realization on standard convex substrates provides an additional degree of freedom for optical designs. Diffraction grating of a spectrometer based on convex substrate allows high spectral and spatial resolution of the entrance slit which yields to high performance of optical system. In fact, for entrance wavefront, diffraction gratings realized on convex substrates are able to diffract, collimate and focus it, simultaneously, in the focal plane [1-4]. They also have the advantages of large field-of-view, compact structure and low distortion of spectral line. So, they are particularly important for some applications such as aero-spatial, geological exploration, environmental monitoring, biochemical analysis, clinical medicine and spaceborne remote sensing, where compact optical system and small volume are required [5]. But, if such diffraction grating can be ruled mechanically on convex substrate, the realization of holographic diffraction grating needs necessarily to prepare a photosensitive layer on a convex substrate before holographic recording, which is a challenge. The details related to the coating process will be developed in the following sections.

Original diffraction grating realization takes generally a long time. Once

master grating has been manufactured according to the ruled or holographic techniques, it can be replicated to produce exact copies of the original. The replication technique has the added advantage of using a single master to produce large quantities of replicas which are then low cost. It is a technique that results in the transfer of the three-dimensional topography of master grating to other substrate, allowing reproduction of master in full relief to extremely close tolerances. As a result, this reliable, cost effective and repeatable process facilitates the widespread use of gratings in various domains, spectroscopic and laser applications.

The reproducibility of replica gratings makes them ideal for high-volume production, and for scientific experiments in which a smaller quantity of absolutely identical gratings is required.

Many techniques of replication have been developed: replica molding [6-8], microtransfer molding [6, 8, 9], microcontact printing [6, 8, 10], micromolding in capillaries [6, 8, 11], solvent-assisted micromolding [6, 8, 12] solvent-vapor-assisted imprinting lithography [13], and microparticule screen printing [14].

The common key element of such replication techniques is an elastomer mold. The most common material used for soft lithographic stamps is made of polydimethylsiloxane (PDMS), a commercially available, thermally curable, and elastomeric polymer [6, 8-10, 14, 15]. According to [8], PDMS has three properties that make it ideal for many applications: (a) It is elastic. One of the primary advantages conferred by elastomeric stamps is the ability to produce patterns on nonplanar substrates. This characteristic, combined with its low surface energy, enables it to make reversible conformal contact with non-planar substrates with minimal applied pressure to curved surfaces. (b) It is mostly transparent down to wavelengths of 280 nm. It can therefore be used as a mold for UV-imprint lithography. (c) It is commercially available in bulk quantities.

And there must be a conformal contact between the PDMS mold, polymer layer, and the substrate. However, due to shear stress during the application of pressure, the edges of the masks can lose conformal contact with substrate [14]. Factors such as molds, solvents, pressure, temperature, duration, and size of the pattern structures can influence the final molded patterns [16]. For replication process using microparticule screen printing, it is important to consider the surfaces properties of the substrates and particles in order to optimize printing efficiency [14]. In the solvent-assisted molding, the solvent molecules diffuse into the polymer thin film as a result of the solvent concentration gradient between the two surfaces, top and bottom [17]. The thickness of a PDMS mold plays an important role in SVAIL process. Rabibrata Mukherjee et al. combined solvent vapor-assisted swelling and patterning of polymers with the idea of using a flexible and water-soluble stamp, to develop an extremely simple, rapid, pressure-less, room temperature patterning technique for high fidelity patterning of films coated on non-planar surfaces [18]. Vinod et al. developed a method which uses macroscopic mechanical deformations of chemically modified silicone films to realize the rational assembly of microscopic polymer structures of various substrates [19].

But to control all those parameters (pression, temperature, mechanical deformation, etc.) at the same time remained a challenge. In our previous work, we realized the replication of a diffraction grating by SVAIL on flat substrate [20]. In the present work, we proposed to replicate a diffraction grating, by SVAIL, on convex substrate. The advantage to realize a diffraction grating on convex substrate is indicated above [1, 5]. We used PDMS mold and we evaluated in real time the diffraction efficiency in the negative first diffraction order, during the replication process. According to theoretical simulations of different steps for SVAIL process, theoretical diffraction efficiency at optimal replication was deduced, and the reference value was predicted to stop the replication process. By performing this monitoring during the replication process, the fundamental question to be answered is the following: "at which moment the replication of the diffraction gratings by SVAIL is it optimal? And the main target of the latter is: "not to extend unnecessarily the replication process, or not to underestimate the duration of the SVAIL process". The other major challenge that must be overcome in this process of diffraction grating replication on convex substrate is the coating of photosensitive layer (photoresist s1805) on the latter. More details related to all these challenges were discussed in the following sections.

Experiment Description

This section describes the replication of a diffraction grating with high fidelity. A commercial diffraction grating, from Thorlabs factory, with known parameters was chosen for commodity: Ruled grating GR13-0605, 12.7 mm x 12.7 mm x 6 mm; 600 lines/mm, blaze angle = 8°37', blaze wavelength = 500 nm [21]. The starting point is the preparation of PDMS mold (Sylgard 184 and curing agent respectively 10:1) of the original diffraction grating. It has been prepared classically as indicated by [15]. The thickness of the PDMS mold was here ±500 µm for more flexibility. Before going on with the replication, let's first talk about photoresist coating on convex substrate.

Spin coating process on curved surfaces

Spin coating is the best way for a uniform coating, particularly for flat substrate. To apply spin coating of thin films on substrates in practice, more experiments and models were built on the basis of Emslie's model, Meyerhofer's model, and Bornside's model [22, 23]. After these models and experiments were reviewed, it was found that they were all suitable for flat surfaces without considering other geometries. The models were suitable for spin coating on spherical surface with a small central angle. When the central angle of a sphere surface is small, the sphere surface is close to a flat surface. This conforms to the prediction in Emslie's paper about spin coating on spherical surfaces with the central angle no larger than 20° [24]. The theoretical research of spin coating was extended to curved surfaces with increasing applications of optical elements including curved gratings [25, 26]. Spin coatings of various types of viscous liquids on curved surfaces have been studied

[27-30]. Spin speed is one of the most important factors in spin coating. Film thickness is largely a balance between the force applied to shear the fluid resin towards the edge of the substrate and the drying rate which affects the viscosity of the resin. As the resin dries, the viscosity increases until the radial force of the spin process can no longer appreciably move the resin over the surface [31]. Film thickness is easily changed by changing spin speed or switching to a different viscosity photoresist. Another advantage of spin coating is the ability of the film to get progressively more uniform as it thins, and if the film ever becomes completely uniform during the coating process. According to Reichle R. et al., spin-coating with standard parameters can produce good photoresist coatings also on the convex surface of a lens in spite of a maximum inclination angle of about 28° at the edge [32]. It means that α ≤28° (Figure 1). The maximum was at α ≤ 20° [24, 33], before reaching that performance.

In fact, in this paper, convex glass substrate coated with

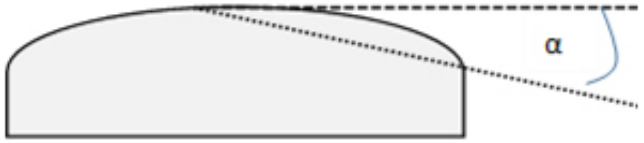

Figure 1: Plano-convex substrate.

photoresist s1805 (from MICROPOSIT® S1800 Shipley Company) was prepared by spin coating. The prepared thickness film was ±300 nm, in agreement with grating groove height h = 250 nm, deduced from given grating parameters. For photoresist coating on convex substrate, the parameters of the spin coater (speed and duration) were of course taken into account according to the desired thickness. In our case, the thickness needed for replication was 300 nm. And to obtain a layer of photoresist s1805 of such thickness (300 nm), spin coating was carried out at a speed of 3500 rpm, for two minutes (Figure 2) [34].

Replication and diffraction efficiency measurement in real time

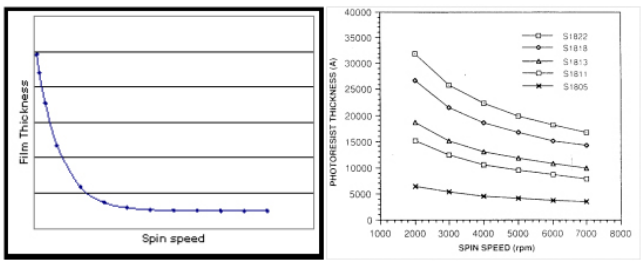

Figure 2: Relation of the spin speed versus film thickness [34].

During the solvent-assisted molding process for example, due to the permeability of the PDMS mold, the solvent is capable to evaporate uniformly and the air bubbles between the interfaces can expel from the mold [15, 16]. The solvent molecules diffuse into the polymer thin film as a result of the solvent concentration gradient between the two surfaces, top and bottom [17]. The thickness of a PDMS mold plays an important role in SVAIL process.

Ethanol was used as solvent. That solvent was conditioned in a glass box. The latter contained at the same time a "small glass box" one. All the two glass boxes were transparent to LASER source @ 532 nm. Plano-convex substrate coated with photoresist s1805 and the PDMS mold in perfect contact were placed inside the small box. The external box (great box) was hermetically sealed, so the solvent gas could not escape, but entered inside the small box. In such conditions, the gas reached the top face of the PDMS mold in perfect contact with photoresist, and the replication process started. Finally, SVAIL process was controlled through diffraction efficiency measured in real time (Figure 3).

The Nd-YAG LASER source (532 nm) used in the

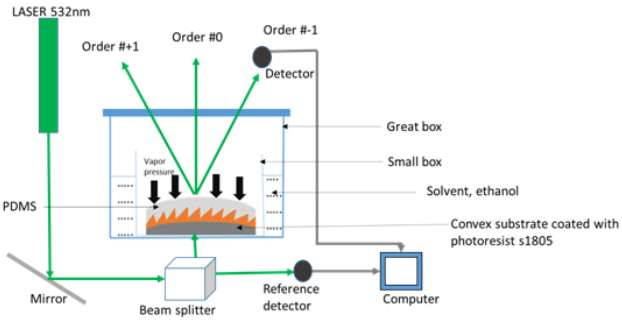

Figure 3: Monitoring set-up of diffraction efficiency during replication process of diffraction grating on convex substrate by SVAIL.

measurement of the diffraction efficiency in real time, was polarized mainly in TE (parallel polarization). And we will base in our theoretical simulations, on the parallel polarization data, shown in the Figure 4, provided by the manufacturer [21], reproduced with permission. Indeed, the qualitative analysis was carried out initially on the basis of observation of the evolution of the diffraction efficiency for several samples: light stability at the first moment (around six first minutes), followed by a sudden drop of diffraction efficiency, and finally

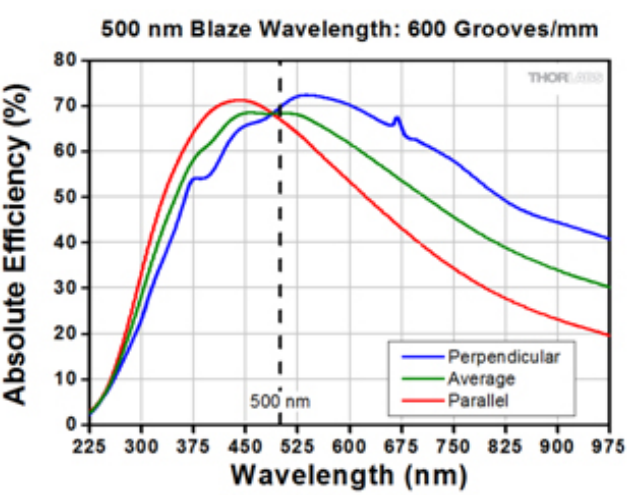

Figure 4: Diffraction efficiency of GR13-0605 (Thorlabs), reproduced with permission.

a slight increase of diffraction efficiency before its stabilization for the rest of the experiment. From these observations, the similarity for these various replicated grating samples emerged. The stability of the LASER source has also been analyzed. This allows us to postulate that the variation of diffraction efficiency was due to the replication process itself; and not to LASER fluctuations. In a second step, knowing the maximum groove height (theoretically 250 nm), we also postulate that the replicated grating has zero groove height at the beginning of the replication process; and groove height was maximum at the end of the optimal replication. The simulation of the diffraction efficiency for these two steps (initial and final) and the intermediate ones make possible to theoretically predict the curve of the diffraction efficiency during the replication process. These theoretical predictions (simulations) curves were then compared to the experimental results obtained in real time.

Results and Discussion

Various parameters of the diffraction grating to be replicated were hereunder.

GR13-0605 parameters: dimensions = 12.7 mm x 12.7 mm x 6 mm; groove density = 600 lines/mm, blaze angle = 8°37', blaze wavelength = 500 nm. Different steps of replication process were theoretically simulated according to commercial PC grate software, taking into account a correlation factor related to the possible real profile obtained after manufacturing which could be different to the ideal profile; so, the manufacturer gave the diffraction efficiency curve obtained according to real groove profile. It means that at 500 nm wavelength, reference to grating's parameters above, ideal groove profile of diffraction grating has normally 82% of theoretical diffraction efficiency, for parallel polarization (TE) (Figure 5). But the manufacturer gave 67% of diffraction efficiency (TE) (Figure 4). Indeed, only the difference of groove profile can explain that discrepancy of diffraction efficiency, so we used a correlation factor and obtained Figure 6, which was similar to that given by Thorlabs manufacturer.

The main steps of the SVAIL replication process (Figure 7) were theoretically simulated (in transmission mode)

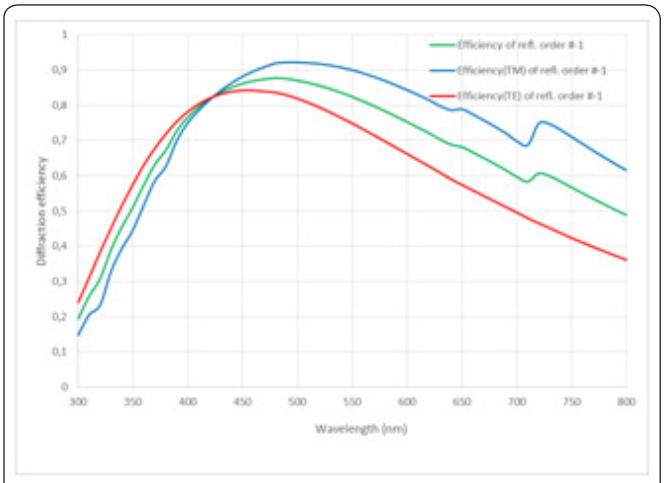

Figure 5: Theoretical diffraction efficiency for 600 lines/mm, blaze angle = 8°37', and blaze wavelength = 500 nm.

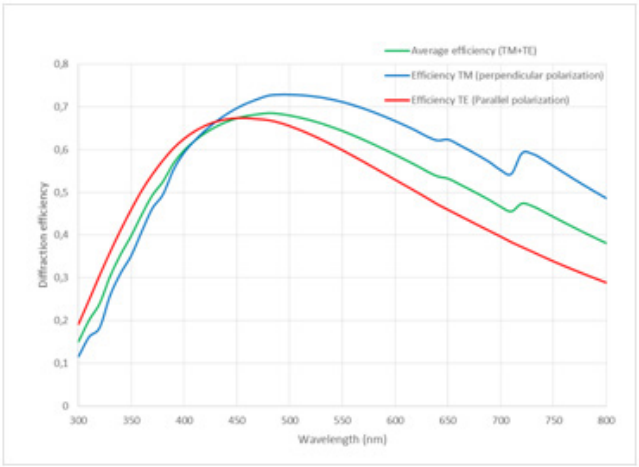

Figure 6: Correlation of diffraction efficiency (estimating real groove profile).

considering the correlation factor; and the results were shown in Figure 8. Even if original diffraction grating was used in reflection mode, theoretical simulations were realized in transmission mode because the monitoring of diffraction efficiency during the replication process was realized in transmission mode (Figure 3).

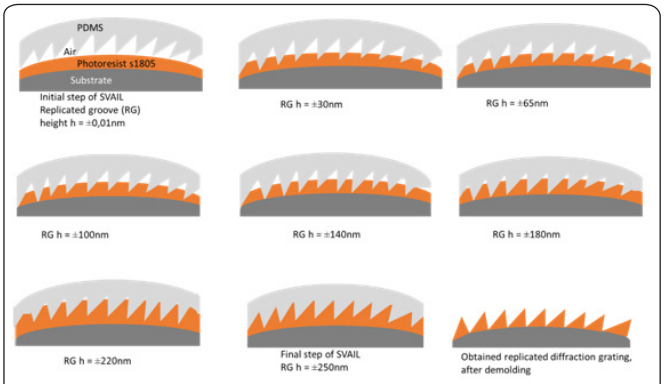

Figure 7: Evolution representation of replicated groove (RG) height during SVAIL replication process.

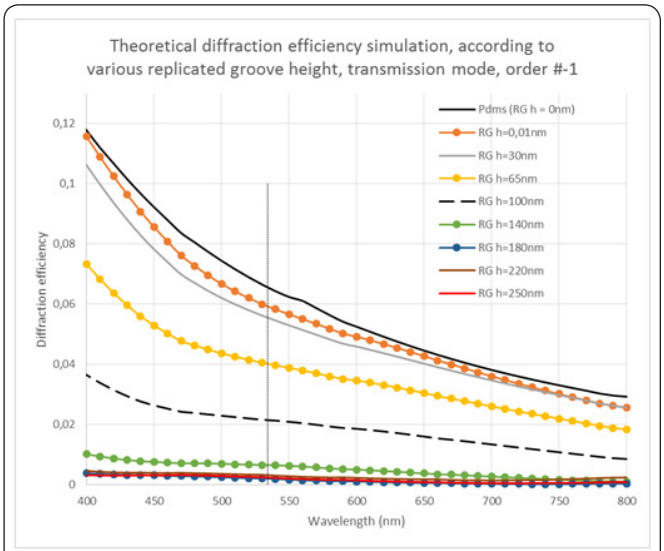

Figure 8: Theoretical simulation of the diffraction efficiency (transmission mode) during SVAIL replication process.

Theoretical variation of the diffraction efficiency, related to various steps of replication process, at 532 nm, was deduced from Figure 8 which covers a large spectral range [400 nm – 800 nm].

Theoretical results at 532 nm, (Figure 9) were compared to experimental results monitored in real time using Nd-YAG LASER @ 532 nm, during the SVAIL replication process, (Figure 10).

As it can be seen in the Figure 10, the SVAIL replication process has three main subdivisions: (a) System stability at the

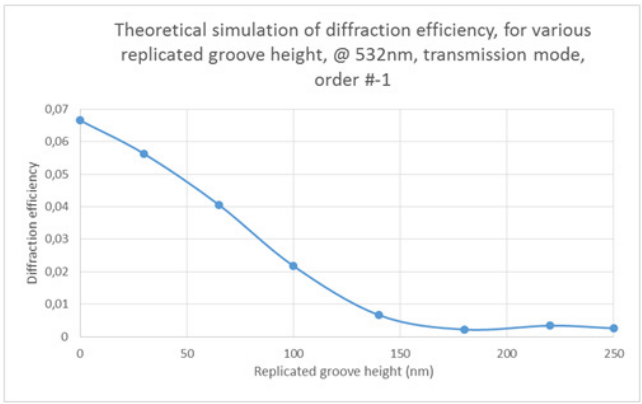

Figure 9: Theoretical simulation of diffraction effficiency, at 532 nm, for various replicated groove height.

first moment of the beginning of replication itself (0 - 400 sec), (b) High activity of replication process where solvent vapor pressure is optimal (450 - 1200 sec), and (c) Searching of final system stability at the last moment of replication process, where it will remain relatively stable (from 1500 sec – end).

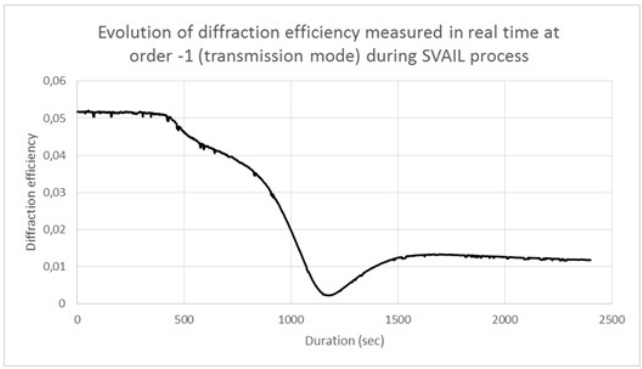

Figure 10: Experimental monitoring of diffraction efficiency during SVAIL replication process.

The inflexion point observed at around 1200 ème sec was maybe related to PDMS elasticity, solvent pressure and the search for system stability. The same behavior was also observed for all samples tested (more than ten samples). The effect of PDMS compression has been theoretically simulated, from 0 nm to 50 nm (50 nm was 20% of total groove height, 250 nm, and that is just an example for illustration).

In fact, if the PDMS was compressed, the groove height decreases, and the diffraction efficiency also decreases. And that was confirmed by theoretical simulation, Figure 11A. At the other side, if the PDMS returns at its initial shape (as elastic), it means zero deformation, the diffraction increases. With Figure 11B, we can represent the PDMS compression - decompression effect (decompression as symmetrical effect of compression) as a function of duration. However, the duration indicated here, Figure 11B was related to the PDMS groove compression – decompression, but not to the replication process duration. In this experimental measurement of diffraction efficiency during replication process, we consider the beginning of PDMS groove deformation due to solvent pressure, at around 1040th sec, and not to 0th sec. We also consider optimal PDMS groove deformation of 50 nm for theoretical simulation.

Any other reason to explain that inflexion point has not

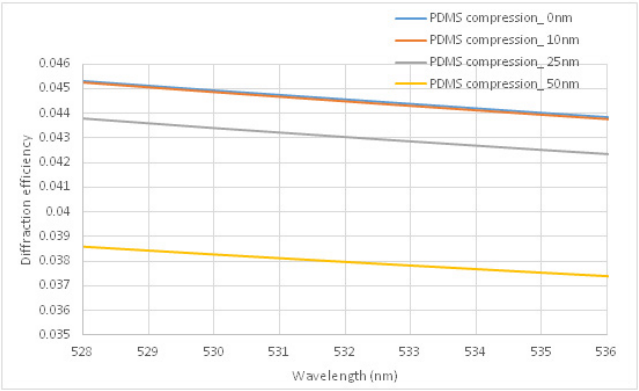

Figure 11A: Theoretical simulation of PDMS compression effect on the diffraction efficiency (here in the first order).

found yet, and we are still looking for it. Finally, different

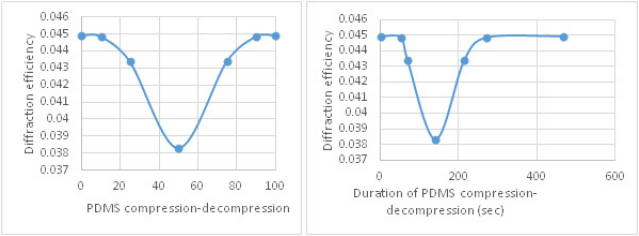

Figure 11B: Theoretical simulation of PDMS compression – decompression effect on the diffraction efficiency.

durations were also tested, and the experimental diffraction efficiency of the replicated grating was concordant to the original grating for all the samples obtained in the final system stability zone.

The combination of Figures 9 and 10 makes possible to deduce the evolution of replicated groove height as a function of duration (Figure 12)

Indeed, in this present case, 40 minutes are enough to realize an optimal diffraction grating replication by SVAIL process. Three replicated gratings have been also fabricated and tested experimentally (Figure 13).

Figure 13 shows a maximal discrepancy of 1.5% (and a minimal of 0.5%) between theoretical and experimental results. That was due to possible measurement errors; or the groove profile used in theoretical simulation was not exactly the same as that used in experimental measurements. And

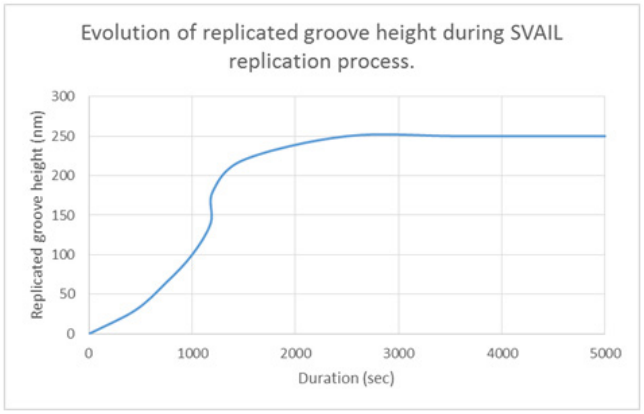

Figure 12: Replicated groove height as a function of duration of SVAIL replication process.

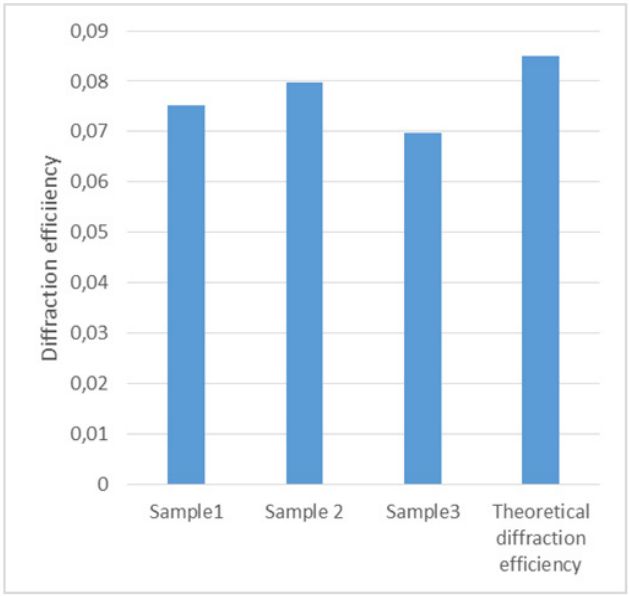

Figure 13: Comparison of diffraction efficiency of replicated gratings measured experimentally and theoretical diffraction efficiency.

that can be seen on the three samples which were replicated in the same conditions, but their experimental measurements of diffraction efficiency were not totally equal. Moreover, two successive experimental measurements of diffraction efficiency for the same diffraction grating are not always identical.

However, even if theoretical simulation of diffraction efficiency for the replicated grating in transmission mode was less than 10%, theoretical simulation of diffraction efficiency in reflectional mode (metallized grating) for the same groove profile was important (Figure 6) and was similar to that provided by the industrial manufacturer (Thorlabs).

Qualitative surface analysis of original and replicated gratings have been done with interferometric microscope at Centre Spatial de Liège (CSL), Figures 14 and 15, to complete the above results.

The global images 3D representation, Figures 14A and 15A, were processed (by MATLAB) to obtain 2D grooves profile and useful for theoretical simulations.

As it can be seen on Figures 14B and 15B, the image acquisition was realized at two different inclinations. The mean

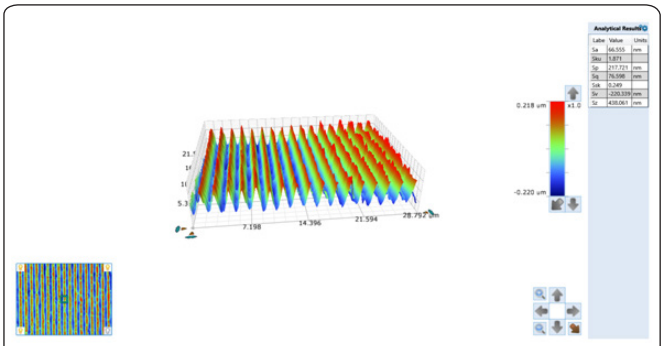

Figure 14A: 3D representation of original (master) grating from Thorlabs, measured at Centre Spatial de Liège (CSL).

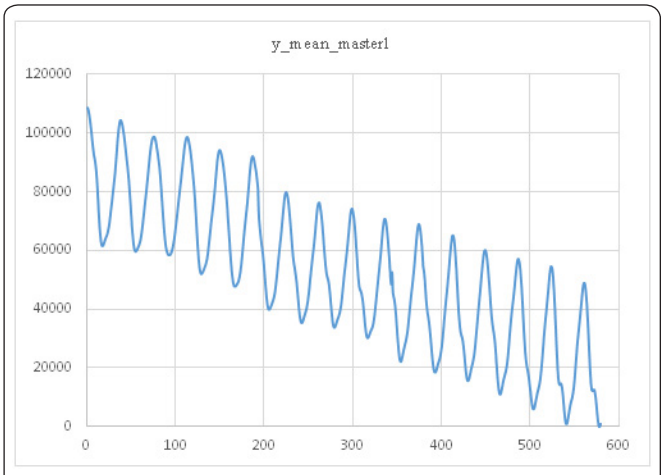

Figure 14B: The mean groove profile of the master grating, over Y-axis.

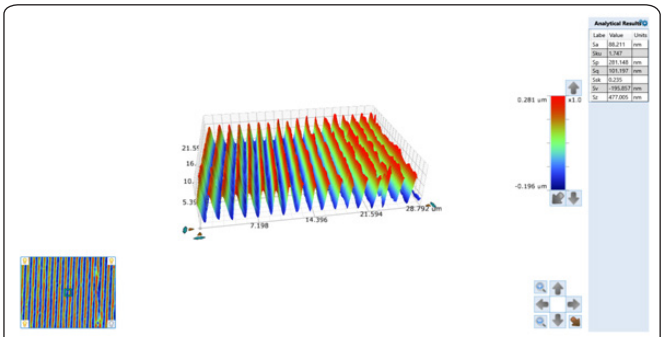

Figure 15A: 3D representation of replicated grating, sample #2, measured at Centre Spatial de Liège (CSL).

profile over X-axis, Figure 16 is obtained with five successive grooves profile for more profile friability. And each mean profile will be used in the following theoretical simulations.

Figure 16 shows that a replicated groove profile can be obtained with a slight left shift of the master groove profile. And the diffraction efficiency of the replicated grating can be obtained with a slight right shift of the diffraction efficiency curve of the master grating (Figure 17). That shift was due to the sample inclination during the profile measurement, and not to the replication process. Finally, reference to the previous results, we can conclude that replication of diffraction grating

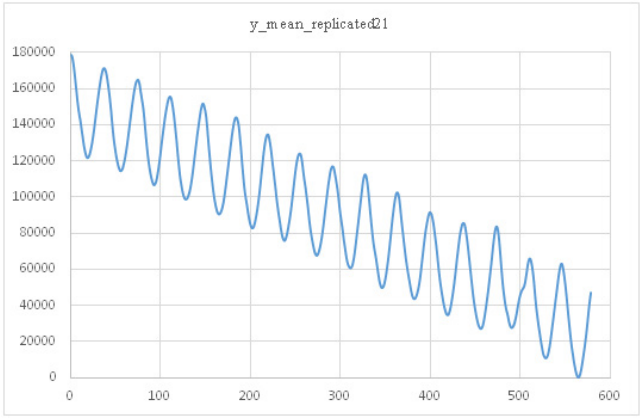

Figure 15B: The mean groove profile of the replicated grating, over Y-axis.

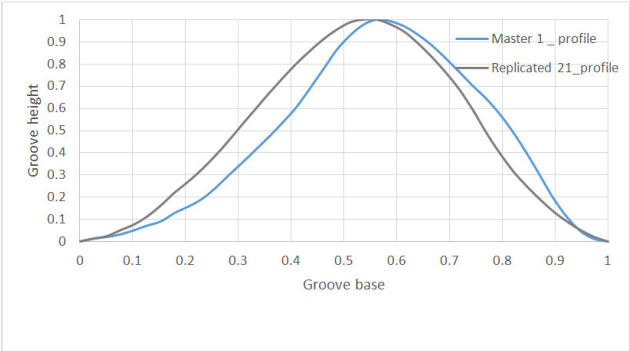

Figure 16: Comparison of measured (real) grooves profile of original (master) and replicated gratings.

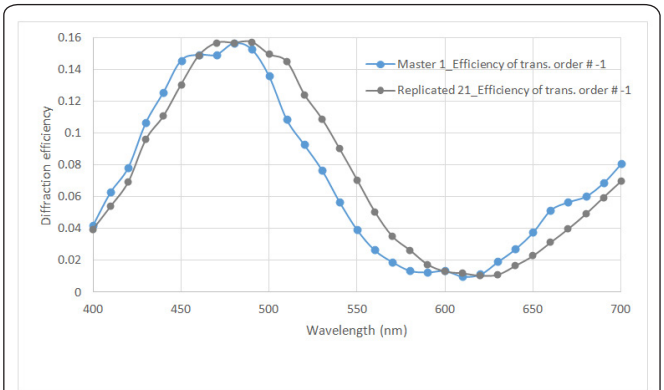

Figure 17: Theoretical simulation of diffraction efficiency according to measured grooves profile of original and replicated gratings.

on convex substrate by SVAIL can be monitored during the replication process, and the obtained results were concordant. Experimental results related to replicated gratings were also concordant to the theory. So, we can finally conclude that the replication fidelity was sufficient.

Conclusion

In this paper, monitoring of diffraction efficiency during the replication of diffraction grating on convex substrate by SVAIL process have been realized. Spin coating of polymer or photoresist on convex substrate have been treated. Monitoring process have been explored, and experimental results have been compared to theoretical simulations for various steps of the replication process. The results were concordant and allowed to indicate the useful duration for optimal diffraction grating replication by SVAIL process; and we obtained a enough fidelity replication. Theoretical simulation of diffraction efficiency according to measured grooves profile (by interferometric microscope) of original and replicated gratings have been realized. The obtained results were concordant, so we can conclude that the SVAIL replication fidelity was sufficient.

Finally, for the replication of a nanostructure of general shape, a diffraction grating which grooves shape (profile) were similar to the latter, can be used as control sample of the nanostructure optimal replication, by controlling the diffraction efficiency of this diffraction grating, in real time.

Acknowledgments

Thanks to Centre Spatial de Liège (Cédric and Lionel) for interferometric microscope measurements.

Funding

The authors received no funding support for this research work.

Conflict of Interest

There are no conflicts of interest to declare.

References

1. Chrisp MP. 1999. Convex diffraction grating imaging spectrometer. U.S. Patent 5,880,834.
2. Davis CO, Bowles J, Leathers RA, Korwan D, Downes TV, et al. 2002. Ocean PHILLS hyperspectral imager: design, characterization, and calibration. *Opt Express* 10(4): 210-221. https://doi.org/10.1364/OE.10.000210
3. Prieto-Blanco X, Montero-Orille C, Couce B, de la Fuente R, et al. 2006. Analytical design of an Offner imaging spectrometer. *Opt Express* 14(20): 9156-9168. https://doi.org/10.1364/OE.14.009156
4. González-Núñez H, Vázquez-Vázquez C, Lago EL, Mouriz MD, Montero-Orille C, et al. 2011. Design, calibration and assembly of an Offner imaging spectrometer. *J Phys Conf Ser* 274(1): 012106. https://www.doi.org/10.1088/1742-6596/274/1/012106
5. Shen C, Tan X, Jiao Q, Zhang W, Wu N, et al. 2018. Convex blazed grating of high diffraction efficiency fabricated by swing ion-beam etching method. *Opt Express* 26(19): 25381-25398. https://doi.org/10.1364/OE.26.025381
6. Xia Y, Whitesides GM. 1998. Soft lithography. *Annu Rev Mater Sci* 28: 153-184. https://doi.org/10.1146/annurev.matsci.28.1.153
7. Xia Y, Kim E, Zhao XM, Rogers JA, Prentiss M, et al. 1996. Complex optical surfaces formed by replica molding against elastomeric masters. *Science* 273(5273): 347-349. https://doi.org/10.1126/science.273.5273.347
8. Lipomi DJ, Martinez RV, Cademartiri L, Whitesides GM. 2012. Soft Lithographic Approaches to Nanofabrication. Matyjaszewski K and Möller M (eds.) Polymer Science: A Comprehensive Reference. Elsevier BV, pp 211-231.

9. Zhao XM, Xia Y, Whitesides GM. 1996. Fabrication of three-dimensional microstructures: microtransfer molding. *Adv Mater* 8(10): 837-840. https://onlinelibrary.wiley.com/doi/abs/10.1002/adma.19960081016
10. Whitesides GM, Kumar A. 1993. Features of gold having micrometer to centimeter dimensions can be formed through a combination of stamping with an elastomeric stamp and an alkanethiol "ink" followed by chemical etching. *Appl Phys Lett* 63(14): 2002-2004.
11. Kim E, Xia Y, Whitesides G. 1995. Polymer microstructures formed by moulding in capillaries. *Nature* 376: 581–584. https://doi.org/10.1038/376581a0
12. King E, Xia Y, Zhao XM, Whitesides GM. 1997. Solvent-assisted microcontact molding: a convenient method for fabricating three-dimensional structures on surfaces of polymers. *Adv Mater* 9(8): 651-654. https://doi.org/10.1002/adma.19970090814
13. Qin D, Xia Y, Whitesides GM. 2010. Soft lithography for micro- and nanoscale patterning. *Nat Protoc* 5(3): 491-502. https://doi.org/10.1038/nprot.2009.234
14. Rose MA, Vinod TP, Morin SA. 2018. Microscale screen printing of large-area arrays of microparticles for the fabrication of photonic structures and for optical sorting. *J Mater Chem C* 6(44): 12031-12037. http://doi.org/10.1039/C8TC02978D
15. Han L, Zhou J, Gong X, Gao CY. 2009. Solvent-assisted polymer micro-molding. *Chin Sci Bull* 54(13): 2193–2204. https://doi.org/10.1007/s11434-009-0212-5
16. Voicu NE, Ludwigs S, Crossland EJW, Andrew P, Steiner U. 2007. Solvent-vapor-assisted imprint lithography. *Adv Mater* 19(5): 757-761. https://doi.org/10.1002/adma.200601599
17. Lai KL, Hon MH, Leu IC. 2011. Pattern formation on polymer resist by solvent-assisted nanoimprinting with PDMS mold as a solvent transport medium. *Micromech Microeng* 21(7): 075013. https://doi.org/10.1088/0960-1317/21/7/075013
18. Mukherjee R, Patil GK, Sharma A. 2009. Solvent vapor-assisted imprinting of polymer films coated on curved surfaces with flexible PVA stamps. *Ind Eng Chem Res* 48(19): 8812-8818. https://doi.org/10.1021/ie801740y
19. Vinod TP, Taylor JM, Konda A, Morin SA. 2016. Stretchable substrates for the assembly of polymeric microstructures. *Small* 13(8): 1603350. https://doi.org/10.1002/smll.201603350
20. Horugavye G, Sabushimike, Habraken S. 2018. Control of solvent vapor assisted imprinting lithography process by real time monitoring of grating diffraction efficiency. *International Journal of Nanotechnology and Applications* 12(1): 1-11.
21. Thorlabs, Inc.
22. Emslie AG, Bonner FT, Peck LG. 1958. Flow of a viscous liquid on a rotating disk. *Journal of Applied Physics* 29(5): 858-862. https://doi.org/10.1063/1.1723300
23. Wang CT, Yen SC. 1995. Theoretical analysis of film uniformity in spinning processes. *Chem Eng Sci* 50(6): 989-999. https://doi.org/10.1016/0009-2509(94)00481-6
24. Gupta VK, Abbott NL. 1997. Design of surfaces for patterned alignment of liquid crystals on planar and curved substrates. *Science* 276(5318): 1533-1536. http://doi.org/10.1126/science.276.5318.1533
25. Feng XG, Sun LC. 2005. Mathematical model of spin-coated photoresist on a spherical substrate. *Opt Express* 13(18): 7070-7075. https://doi.org/10.1364/OPEX.13.007070
26. Chen LJ, Liang YY, Luo JB, Zhang CH, Yang GG. 2009. Mathematical modeling and experimental study on photoresist whirl-coating in convex-surface laser lithography. *J Opt A: Pure Appl Opt* 11(10): 105408. https://doi.org/10.1088/1464-4258/11/10/105408
27. Brytsche HH, Farley ED, White SS. 1998. Method for spin coating a multifocal lens. U.S. Patent 5,753,301.
28. Blackburn WP, Bowles RJ, Levesque MB, Maldonado E. 2002. Spin and spray coating process for curved surfaces. U.S. Patent 6, 352,747.
29. Brassard JD, Sarkar DK, Perron J. 2012. Fluorine based superhydrophobic coatings. *Appl Sci* 2(2): 453-464. https://doi.org/10.3390/app2020453
30. Acrivos A, Shah MJ, Petersen EE. 1960. On the flow of a non-newtonian liquid on a rotating disk. *Journal of Applied Physics* 31(6): 963-968. https://doi.org/10.1063/1.1735785
31. Tyona MD. 2013. A theoretical study on spin coating technique. *Advances in Materials Research*. 2(4): 195-208. https://doi.org/10.12989/amr.2013.2.4.195
32. Reichle R, Yu K, Pruss C, Osten W. 2008. Spin-coating of photoresist on convex lens substrates. *DGaO Proceedings* 109: P44.
33. Hall DB, Underhill P, Torkelson JM. 1998. Spin coating of thin and ultrathin polymer films. *Polymer Engineering and Science* 38(12): 2039-2045. https://doi.org/10.1002/pen.10373
34. Shipley Company, Microposit® S1800® Series Photo Resists.